

Prof. Yu Huang
State Key Lab of Loess and Quaternary Geology
Institute of Earth Environment, Chinese Academy
of Sciences, Xi'an, 710061, China
Tel./Fax: (86) 29-62336261
E-mail: huangyu@ieecas.cn

Jan. 27, 2022

Dear reviewer,

Revision for Manuscript acp-2021-890

We thank you very much for giving us the opportunity to revise our manuscript. We highly appreciate the reviewer for their comments and suggestions on the manuscript entitled “**OH-initiated atmospheric degradation of hydroxyalkyl hydroperoxides: mechanism, kinetics, and structure-activity relationship**”. We have made revisions of our manuscript carefully according to the comments and suggestions of reviewer. The revised contents are marked in blue color. The response letter to reviewer is attached at the end of this cover letter.

We hope that the revised manuscript can meet the requirement of Atmospheric Chemistry & Physics. Any further modifications or revisions, please do not hesitate to contact us.

Look forward to hearing from you as soon as possible.

Best regards,

Yu Huang

Comments of reviewer #1

1. The investigated HHPs are generated from the reactions of CH_2OO , *anti*- CH_3CHOO and $(\text{CH}_3)_2\text{COO}$ with water vapor, not considering the HHP from the bimolecular reaction of *syn*- CH_3CHOO with water. This should be stated.

Response: Based on the Reviewer's suggestion, OH-initiated oxidation of hydroxyalkyl hydroperoxide (HHP), generated from the bimolecular reaction of *syn*- CH_3CHOO with water, has been added in the revised manuscript. The corresponding free-energy and electronic-energy potential energy surface (PES) are displayed in Figures S4 and S5, respectively. As shown in Figure S4, the H-abstraction by OH radical from $\text{HOCH}(\text{CH}_3)\text{OOH}$ has six kinds of pathways. For each pathway, a pre-reactive complex is formed prior to the corresponding transition state, and then it overcomes modest barrier to reaction. The ΔG_a^\ddagger of R6' and R8' are 2.3 and 1.8 kcal mol^{-1} , respectively, which are $\sim 5 \text{ kcal mol}^{-1}$ lower than those of R5' and R7'. This result shows that H-abstraction from the -CH (R6') and -OOH (R8') groups are preferable kinetically. Same conclusion is also derived from the energy barriers ΔE_a^\ddagger that R6' and R8' the most favourable H-abstraction pathways (Figure S5). It should be noted that although the barriers of R6' and R8' are comparable, the exoergicity of the former case is significantly lower than that of the latter case. The above-mentioned conclusions are consistent with the results derived from the OH-initiated oxidation of $\text{HOCH}(\text{CH}_3)\text{OOH}$ from the *anti*- $\text{CH}_3\text{CHOO} + \text{H}_2\text{O}$ reaction. Zhou et al. has demonstrated that the bimolecular reaction of *syn*- CH_3CHOO with water leading to the formation of $\text{HOCH}(\text{CH}_3)\text{OOH}$ is of less importance in the atmosphere, while the unimolecular decay to OH radical is the major loss process of *syn*- CH_3CHOO (Zhou et al., 2019). Therefore, in the present study, we mainly focus on the subsequent mechanism of intermediate generated from OH-initiated oxidation of $\text{HOCH}(\text{CH}_3)\text{OOH}$ from the *anti*- $\text{CH}_3\text{CHOO} + \text{H}_2\text{O}$ reaction.

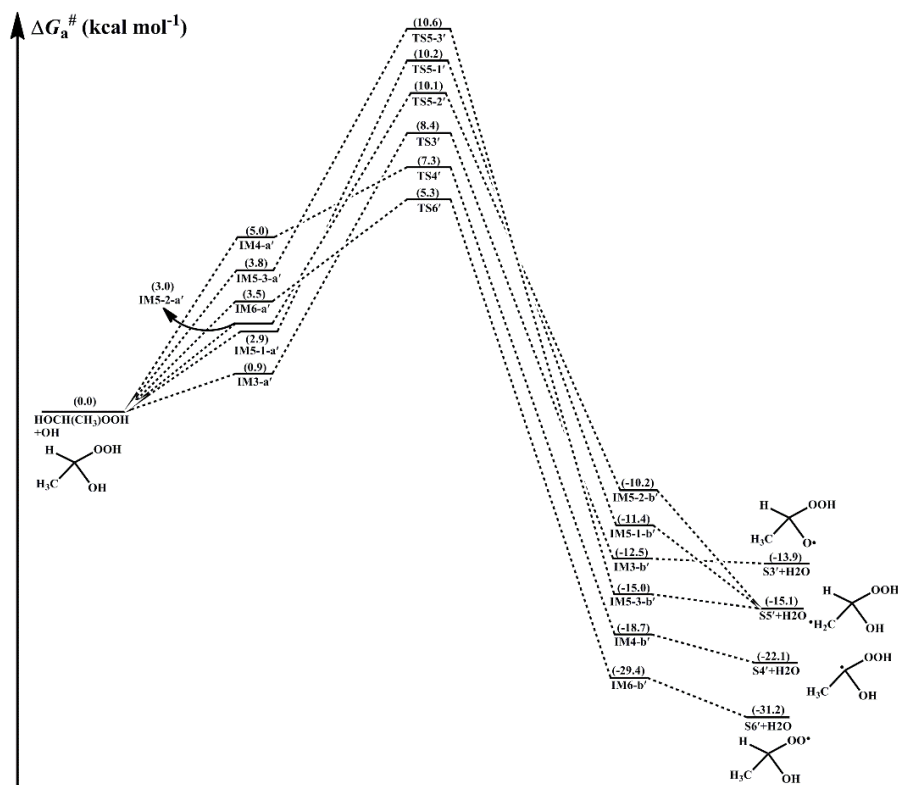


Figure S4. PES (ΔG_a^\ddagger) for the OH-initiated reactions of HOCH(CH₃)OOH from the *syn*-CH₃CHOO + H₂O reaction predicted at the M06-2X/ma-TZVP//M06-2X/6-311+G(2df,2p) level of theory (a and b represent the pre-reactive and post-reactive complexes)

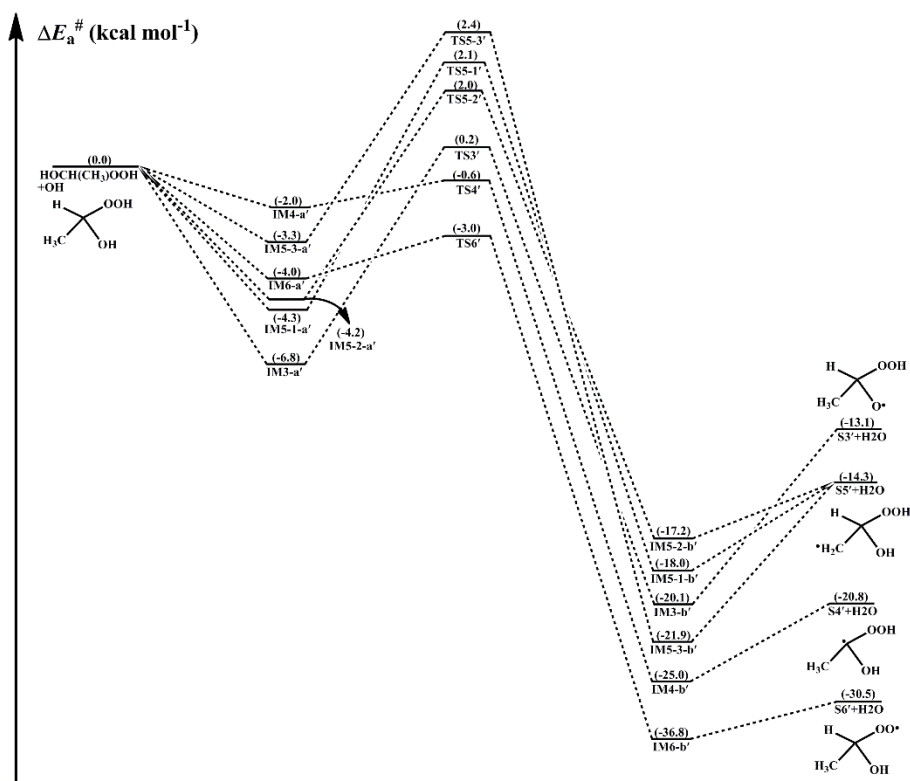


Figure S5. PES (ΔE_a^\ddagger) for the OH-initiated reactions of HOCH(CH₃)OOH from the *syn*-CH₃CHOO + H₂O reaction predicted at the M06-2X/ma-TZVP//M06-2X/6-311+G(2df,2p) level of theory (a and b represent the pre-reactive and post-reactive complexes)

Corresponding descriptions have been added in the page 11 line 289-308 of the revised manuscript:

For the OH-initiated oxidation of HOCH(CH₃)OOH from the syn-CH₃CHOO + H₂O reaction, the corresponding free-energy and electronic-energy PESs are displayed in Figures S4 and S5, respectively. From Figure S4, it can be seen the H-abstraction by OH radical from HOCH(CH₃)OOH has six kinds of pathways. For each pathway, a pre-reactive complex is formed prior to the corresponding transition state, and then it overcomes modest barrier to reaction. The ΔG_a^\ddagger of R6' and R8' are 2.3 and 1.8 kcal mol⁻¹, respectively, which are about 5 kcal mol⁻¹ lower than those of R5' and R7'. This result shows that H-abstraction from the -CH (R6') and -OOH (R8') groups are preferable kinetically. Same conclusion is also derived from the energy barriers ΔE_a^\ddagger that the R6' and R8' the most favourable H-abstraction pathways (Figure S5). It should be noted that although the barriers of R6' and R8' are comparable, the exoergicity of the former case is significantly lower than that of the latter case. The above-mentioned conclusions are consistent with the results derived from the OH-initiated oxidation of HOCH(CH₃)OOH from the anti-CH₃CHOO + H₂O reaction. Zhou et al. has demonstrated that the bimolecular reaction of syn-CH₃CHOO with water leading to the formation of HOCH(CH₃)OOH is of less importance in the atmosphere, while the unimolecular decay to OH radical is the major loss process of syn-CH₃CHOO (Zhou et al., 2019). Therefore, in the present study, we mainly focus on the subsequent mechanism of intermediate generated from OH-initiated oxidation of HOCH(CH₃)OOH from the anti-CH₃CHOO + H₂O reaction.

2. Line 226-228, the reaction barriers are reduced in the order of 6.4 (R1) > 5.8 (R3) \approx 5.4 (R2) > 1.5 (R4) kcal mol⁻¹, indicating that H-abstraction from the -OOH group is the most favorable. The authors should explain the order of TS1, TS3, TS2, and TS4 in the initial H-abstraction reactions.

Response: Based on the Reviewer's suggestion, the corresponding explanations on the order of barrier heights of H-abstraction reactions have been added in the revised manuscript. A schematic PES for the initiation reactions of OH radical with HOCH₂OOH is drawn in Figure 2. As can be seen in Figure 2, the reaction for HOCH₂OOH with OH radical proceeds via four distinct pathways: H-abstraction from the -O₁H₁ (R1), -C₁H₃ (R2), -C₁H₄ (R3) and -O₂O₃H₂ groups (R4). For each pathway, a pre-reactive complex with a six- or seven-membered ring

structure is formed in the entrance channel, which is stabilized by hydrogen bond interactions between the oxygen atom of OH radical and the abstraction hydrogen atom of HOCH₂OOH, and the remnant hydrogen atom of OH radical and one of oxygen atoms of HOCH₂OOH. Then, it surmounts modest barrier that is higher in energy than the reactants to reaction. The reaction barrier ΔG_a^\ddagger are reduced in the order of 6.4 (R1) > 5.8 (R2) \approx 5.4 (R3) > 1.5 (R4) kcal mol⁻¹, indicating that H-abstraction from the -O₂O₃H₂ group (R4) is more preferable than those from the -O₁H₁, -C₁H₃ and -C₁H₄ groups (R1-R3). Same conclusion is also derived from the energy barriers ΔE_a^\ddagger that R4 is the most favorable H-abstraction pathway (Figure S1). The difference of barrier heights can be attributed to the bond dissociation energy (BDE) of different types of bonds in HOCH₂OOH molecule. The BDE are decreased in the order of 103.7 (O₁-H₁) > 98.2 (C₁-H₃) \approx 97.4 (C₁-H₄) > 87.2 (O₃-H₂) kcal mol⁻¹, which are in good agreement with the order of barrier heights of H-abstraction reactions.

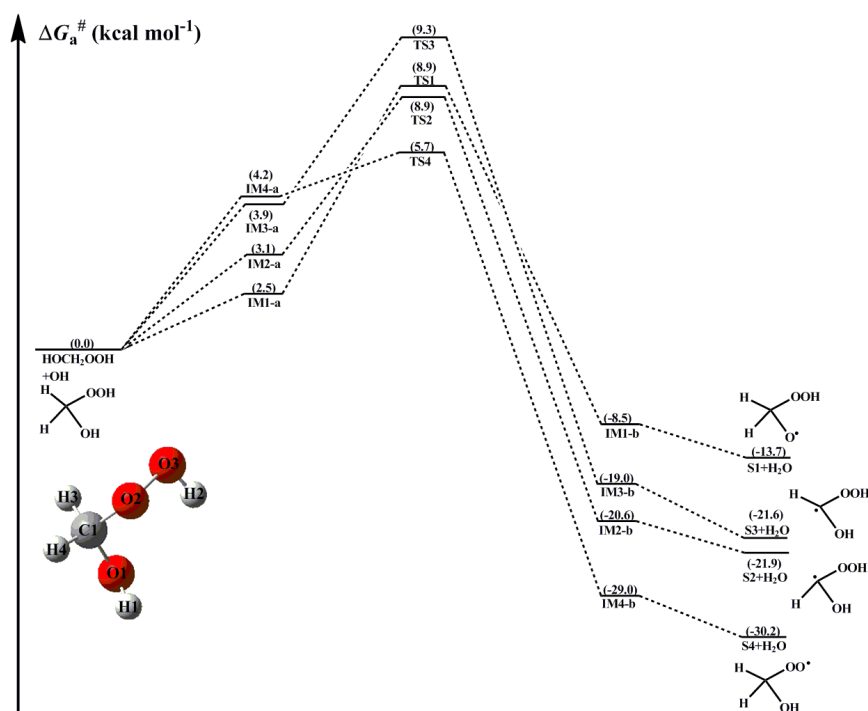


Figure 2. PES (ΔG_a^\ddagger) for the OH-initiated reactions of HOCH₂OOH from the CH₂OO + H₂O reaction predicted at the M06-2X/ma-TZVP//M06-2X/6-311+G(2df,2p) level of theory (a and b represent the pre-reactive and post-reactive complexes)

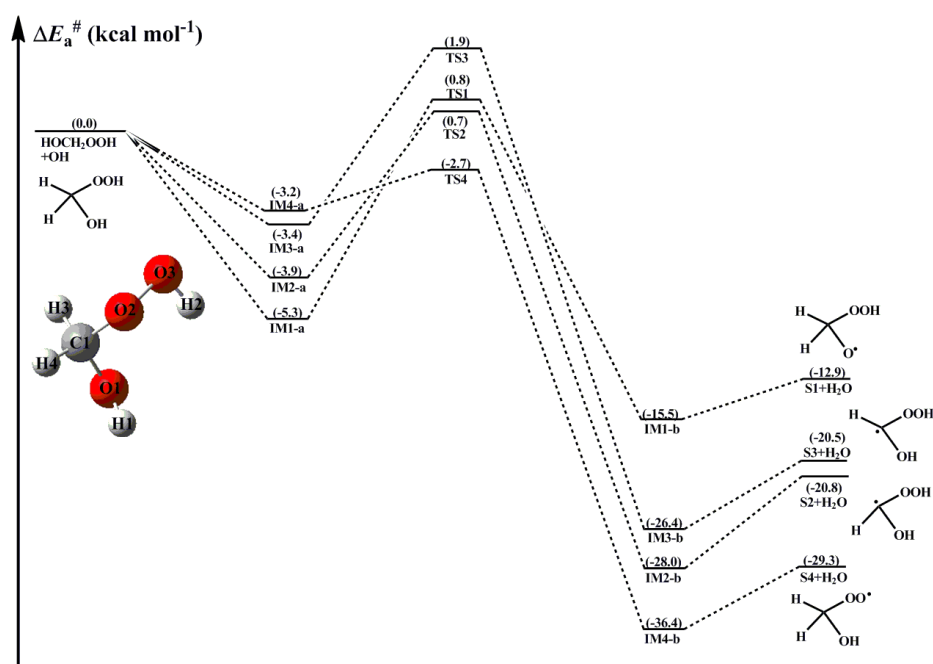


Figure S1. PES (ΔE_a^\ddagger) for the OH-initiated reactions of HOCH₂OOH from the CH₂OO + H₂O reaction predicted at the M06-2X/ma-TZVP//M06-2X/6-311+G(2df,2p) level of theory (a and b represent the pre-reactive and post-reactive complexes)

Corresponding descriptions have been added in the page 10 line 253-269 of the revised manuscript:

As can be seen in Figure 2, the reaction for HOCH₂OOH with OH radical proceeds via four distinct pathways: H-abstraction from the -O₁H₁ (R1), -C₁H₃ (R2), -C₁H₄ (R3) and -O₂O₃H₂ groups (R4). For each pathway, a pre-reactive complex with a six- or seven-membered ring structure is formed in the entrance channel, which is stabilized by hydrogen bond interactions between the oxygen atom of OH radical and the abstraction hydrogen atom of HOCH₂OOH, and the remnant hydrogen atom of OH radical and one of oxygen atoms of HOCH₂OOH. Then, it surmounts modest barrier that is higher in energy than the reactants to reaction. The reaction barrier ΔG_a^\ddagger are reduced in the order of 6.4 (R1) > 5.8 (R2) \approx 5.4 (R3) > 1.5 (R4) kcal mol⁻¹, indicating that H-abstraction from the -O₂O₃H₂ group (R4) is more preferable than those from the -O₁H₁, -C₁H₃ and -C₁H₄ groups (R1-R3). Same conclusion is also derived from the energy barriers ΔE_a^\ddagger that R4 is the most favorable H-abstraction pathway (Figure S1). The difference of barrier heights can be attributed to the bond dissociation energy (BDE) of different types of bonds in HOCH₂OOH molecule. The BDE are decreased in the order of 103.7 (O₁-H₁) > 98.2 (C₁-H₃) \approx 97.4 (C₁-H₄) > 87.2 (O₃-H₂) kcal mol⁻¹, which are in good agreement with the order of barrier heights of H-abstraction reactions.

3. The authors discuss the mechanism of RO₂ reactions with HO₂. But there is no information provided on HO₂. They must describe how HO₂ is formed in the atmosphere, what is its concentration, and where this reaction could be relevant.

Response: Based on the Reviewer's suggestion, the relevant information on the production of HO₂ radical has been added in the revised manuscript. The main sources of HO₂ radical involve the photo-oxidation of oxygenated volatile organic compounds (OVOCs) and the ozonolysis reaction, as well as secondary sources include the reactions of OH radical with CO, ozone and volatile organic compounds (VOCs), the reaction of alkoxy radical RO with O₂ and the red-light-induced decomposition of α-hydroxy methylperoxy radical OHCH₂OO (Stone et al., 2012; Hofzumahaus et al., 2009; Kumar et al., 2015). The atmospheric concentration of HO₂ radical is $1.5-10 \times 10^8$ molecules cm⁻³ at ground level in polluted urban environments (Stone et al., 2012).

Corresponding descriptions have been added in the page 21 line 496-503 of the revised manuscript:

The main sources of HO₂ radical involve the photo-oxidation of oxygenated volatile organic compounds (OVOCs) and the ozonolysis reaction, as well as secondary sources include the reactions of OH radical with CO, ozone and volatile organic compounds (VOCs), the reaction of alkoxy radical RO with O₂ and the red-light-induced decomposition of α-hydroxy methylperoxy radical OHCH₂OO (Kumar et al., 2015; Stone et al., 2012; Hofzumahaus et al., 2009). The atmospheric concentration of HO₂ radical is $1.5-10 \times 10^8$ molecules cm⁻³ at ground level in polluted urban environments (Stone et al., 2012).

4. Authors should compare k_{MC-TST} and the pseudo first-order rates (k'_{HO_2} and k'_{NO}) for the bimolecular processes (HO₂ reaction and NO reaction) as a function of concentration. See the recent review of autoxidation by Bianchi et al. (Chem. Rev. 2019, 119, 6, 3472-3509).

Response: As the Reviewer's said, the relative importance of different transformation pathways (unimolecular, HO₂· and NO reactions) of peroxy radicals RO₂ is significantly dependent on the rate coefficients and coreactant concentrations. For the H-shift reaction of RO₂ radicals, the multi-conformer rate coefficient k_{MC-TST} can be calculated by the weighted sum of the single-conformer rate coefficient k_{RC-TST} . At room temperature, k_{MC-TST} of first H-shift reaction of

HOCH₂OO radical is calculated to be $4.4 \times 10^{-16} \text{ s}^{-1}$. The room temperature rate coefficient of HOCH₂OO radical reaction with HO₂ radical is estimated to be $1.7 \times 10^{-11} \text{ cm}^3 \text{ molecule}^{-1} \text{ s}^{-1}$. The typical atmospheric concentrations of HO₂ radical are 5, 20 and 50 pptv in the urban, rural and forest environments (Bianchi et al., 2019), translating into the pseudo-first-order rate constants $k'_{\text{HO}_2} = k_{\text{HO}_2}[\text{HO}_2]$ of 1.1×10^{-3} , 4.2×10^{-3} and $1.1 \times 10^{-2} \text{ s}^{-1}$, respectively.

The typical atmospheric concentrations of NO are about 10 ppbv, 1 ppbv and 20 pptv in the urban, rural and forest environments (Bianchi et al., 2019). The rate coefficient of HOCH₂OO radical reaction with NO is calculated to be $4.3 \times 10^{-12} \text{ cm}^3 \text{ molecule}^{-1} \text{ s}^{-1}$ at room temperature, resulting in the pseudo-first-order rate constants $k'_{\text{NO}} = k_{\text{NO}}[\text{NO}]$ of 6.5×10^{-1} , 6.5×10^{-2} , and 1.3×10^{-3} , respectively, in the urban, rural and forest environments. It is of interest to assess the relative importance for the H-shift reaction of HOCH₂OO radical and bimolecular reactions with HO₂· and NO based on the calculated $k_{\text{MC-TST}}$, k'_{HO_2} and k'_{NO} . It can be found that the H-shift reaction is of less importance, the HO₂ radical reaction is favourable in the forest environment, the NO reaction is predominant in the urban and rural regions. Similar conclusion is also obtained from the cases of HOCH(CH₃)OO and HO(CH₃)₂CHOO radicals.

Corresponding descriptions have been added in the page 22 line 525-531 and page 27 line 653-664 of the revised manuscript:

At ambient temperature, k_{R31} is estimated to be $1.7 \times 10^{-11} \text{ cm}^3 \text{ molecule}^{-1} \text{ s}^{-1}$, which is in good agreement with the value of $\sim 2 \times 10^{-11} \text{ cm}^3 \text{ molecule}^{-1} \text{ s}^{-1}$ for the reaction of acyl peroxy radicals with HO₂ radical (Wennberg et al., 2018). The typical atmospheric concentrations of HO₂ radical are about 5, 20 and 50 pptv in the urban, rural and forest environments (Bianchi et al., 2019), translating into the pseudo-first-order rate constants $k'_{\text{HO}_2} = k_{\text{HO}_2}[\text{HO}_2]$ of 1.1×10^{-3} , 4.2×10^{-3} and $1.1 \times 10^{-2} \text{ s}^{-1}$, respectively.

The typical atmospheric concentrations of NO are about 10 ppbv, 1 ppbv and 20 pptv in the urban, rural and forest environments (Bianchi et al., 2019). The rate coefficient of HOCH₂OO· reaction with NO is calculated to be $4.3 \times 10^{-12} \text{ cm}^3 \text{ molecule}^{-1} \text{ s}^{-1}$ at room temperature, resulting in the pseudo-first-order rate constants $k'_{\text{NO}} = k_{\text{NO}}[\text{NO}]$ of 6.5×10^{-1} , 6.5×10^{-2} , and 1.3×10^{-3} , respectively, in the urban, rural and forest environments. It is of interest to assess the relative importance for the H-shift reaction of HOCH₂OO radical and bimolecular reactions with HO₂· and NO based on the calculated $k_{\text{MC-TST}}$, k'_{HO_2} and k'_{NO} . It can be found that

the H-shift reaction is of less importance, the HO₂ radical reaction is favorable in the forest environment, while the NO reaction is predominant in the urban and rural regions. Similar conclusion is also obtained from the cases of HOCH(CH₃)OO and HO(CH₃)₂CHOO radicals.

5. For the alkoxy radical fragmentation, the author should calculate rate constants in the temperature range studied.

Response: Based on the Reviewer's suggestion, the rate coefficients of the dominant pathways of alkoxy radical fragmentation have been calculated over the temperature range of 273-400 K. The corresponding results are listed in Table S12 of the revised manuscript. For the fragmentation of HOCH₂O radical, the dominant pathway is H-abstraction by O₂ from HOCH₂O radical resulting in formation of HCOOH and HO₂ radical (R41). For the fragmentation of HOCH(CH₃)O and HOC(CH₃)₂O radicals, the dominant pathways are β-site C-C bond scission leading to the formation of HCOOH + CH₃· (R45) and CH₃COOH + CH₃· (R51). As can be seen in Table S12, k_{R41} is slightly increased with the temperature increasing, and the discrepancy is about a factor of 12 at the two extremes of temperature. At ground level with [O₂] = ~ 5.0 × 10¹⁸ molecule cm⁻³, the pseudo-first-order rate constant $k'_{O_2} = k_{R41}[O_2]$ is estimated to be 38.0 s⁻¹ at room temperature. k_{R45} vary significantly from 2.0 × 10⁶ (273 K) to 3.1 × 10⁸ (400 K) s⁻¹, and they exhibit a marked positive temperature dependence. Similar phenomenon is also observed from k_{R51} that k_{R51} is significantly increased with the temperature increasing. k_{R51} is a factor of ~ 1.3 greater than k_{R45} in the temperature range studied, implying that the rate coefficient of β-site C-C bond scission is slightly increased as the number of methyl group is increased.

Table S12 Rate coefficients of the dominant pathways of the fragmentation of HOCH₂O· (R41), HOCH(CH₃)O· (R45) and HO(CH₃)₂CO· (R51) computed at different temperatures

T/K	$k_{R41}(\text{cm}^3 \text{ molecule}^{-1} \text{ s}^{-1})$	$k_{R45}(\text{s}^{-1})$	$k_{R51}(\text{s}^{-1})$
273	4.3×10^{-18}	2.0×10^6	2.6×10^6
280	5.0×10^{-18}	2.9×10^6	3.8×10^6
298	7.6×10^{-18}	7.3×10^6	9.5×10^6
300	7.9×10^{-18}	8.1×10^6	1.0×10^7
320	1.2×10^{-17}	1.9×10^7	2.5×10^7
340	1.8×10^{-17}	4.4×10^7	5.6×10^7
360	2.6×10^{-17}	9.0×10^7	1.1×10^8

380	3.7×10^{-17}	1.7×10^8	2.2×10^8
400	5.1×10^{-17}	3.1×10^8	3.8×10^8

Corresponding descriptions have been revised in the page 26 line 625-629, page 27 line 633-640, page 27 line 648-652 and page 28 line 655-675 of the revised manuscript:

The formed HOCH₂O radical has two kinds of pathways: (1) it directly decomposes into CH₂O and OH radical (R40) via β -site C₁-O₁ bond scission with the barrier of 52.4 kcal mol⁻¹; (2) it converts into HCOOH and HO₂ radical (R41) through H-abstraction by O₂ with the barrier of 26.4 kcal mol⁻¹. This result reveals that R41 is the most feasible channel in the fragmentation of HOCH₂O radical.

The resulting HOCH(CH₃)O radical has three types of pathways. The first one is β -site C₁-C₂ bond scission leading to the formation of HCOOH + CH₃ (R45) with the barrier of 8.3 kcal mol⁻¹. The second one is β -site C₁-O₁ bond cleavage resulting in formation of CH₃COH + OH (R46) with the barrier of 26.7 kcal mol⁻¹. The third one is H-abstraction by O₂ leading to CH₃COOH + HO₂ (R47) with the barrier of 26.2 kcal mol⁻¹. Based on the calculated reaction barriers, it can be found that β -site C₁-C₂ bond scission is the dominant pathway in the fragmentation of HOCH(CH₃)O radical.

The formed HO(CH₃)₂CO radical can either dissociate to CH₃COOH + CH₃ (R51) via the C₁-C₃ bond scission with the barrier of 8.2 kcal mol⁻¹, or decompose into CH₃COCH₃ + OH (R52) through the C₁-O₁ bond breaking with the barrier of 24.3 kcal mol⁻¹. The result again shows that the β -site C-C bond scission is the dominate pathway.

The rate coefficients of the dominant pathways of HOCH₂O, HOCH(CH₃)O and HO(CH₃)₂CHO radicals fragmentation are summarized in Table S12. As can be seen in Table S12, k_{R41} is slightly increased with the temperature increasing, and the discrepancy is about a factor of 12 at the two extremes of temperature. At ground level with [O₂] = $\sim 5.0 \times 10^{18}$ molecule cm⁻³, the pseudo-first-order rate constant $k'_{O_2} = k_{R41}[O_2]$ is estimated to be 38.0 s⁻¹ at room temperature. k_{R45} vary significantly from 2.0×10^6 (273 K) to 3.1×10^8 (400 K) s⁻¹, and they exhibit a marked positive temperature dependence. Similar phenomenon is also observed from k_{R51} that k_{R51} is significantly increased with increasing temperature. k_{R51} is a factor of ~ 1.3 greater than k_{R45} in the temperature range studied, implying that the rate coefficient of β -site C-C bond scission is slightly increased as the number of methyl group is increased.

6. The prefix 'anti' should be italicized throughout the manuscript.

Response: Based on the Reviewer's suggestion, the prefix 'anti' is italicized throughout the manuscript.

7. The italics/non-italics energies in Fig. S13 and S14 in the supplement are not always in the same vertical order.

Response: Based on the Reviewer's suggestion, the non-italics energies have been placed in the upper number in Figures S13 and S14.

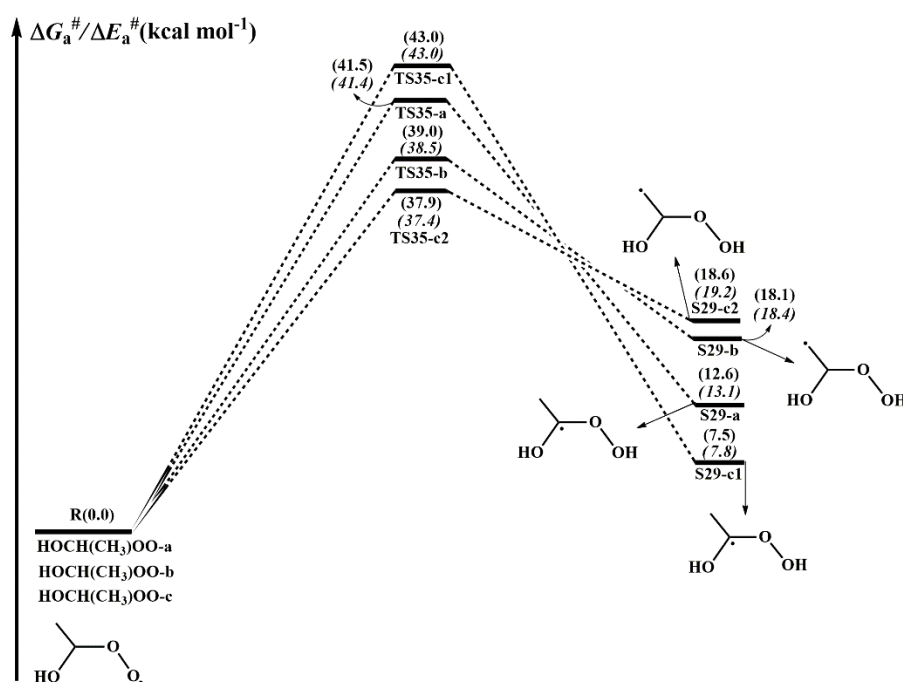


Figure S13. PES (ΔG_a^\ddagger and ΔE_a^\ddagger , in italics) for the autoxidation of HOCH₂CHOO radical predicted at the M06-2X/ma-TZVP//M06-2X/6-311+G(2df,2p) level of theory

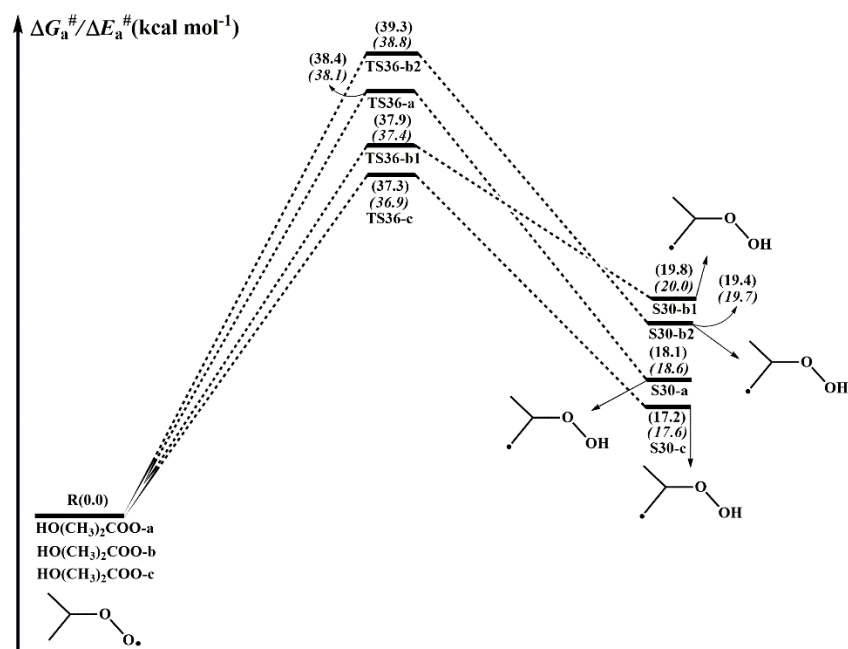


Figure S14. PES (ΔG_a^\ddagger and ΔE_a^\ddagger , in italics) for the autoxidation of HO(CH₂)₂COO radical predicted at the M06-2X/ma-TZVP//M06-2X/6-311+G(2df,2p) level of theory

8. There are some grammatical and logical errors in this manuscript. I suggest revising the grammatical errors accordingly.

Response: Based on the Reviewer's suggestion, the sentences/phrases, missing words, and the grammatically confusing sentences have been corrected carefully in the revised manuscript.

References

1. Zhou, X., Liu, Y., Dong, W., and Yang, X.: Unimolecular reaction rate measurement of *syn*-CH₃CHOO, *J. Phys. Chem. Lett.*, 10, 4817-4821, <https://doi.org/10.1021/acs.jpcclett.9b01740>, 2019.
2. Stone, D., Whalley, L. K., and Heard, D. E.: Tropospheric OH and HO₂ radicals: field measurements and model comparisons, *Chem. Soc. Rev.*, 41, 6348-6404, <https://doi.org/10.1039/c2cs35140d>, 2012.
3. Hofzumahaus, A., Rohrer, F., Lu, K., Bohn, B., Brauers, T., Chang, C. C., Fuchs, H., Holland, F., Kita, K., Kondo, Y., Li, X., Lou, S., Shao, M., Zeng, L., Wahner, A., and Zhang, Y.: Amplified trace gas removal in the troposphere, *Science*, 324, 1702-1704, <https://doi.org/10.1126/science.1164566>, 2009.
4. Kumar, M., and Francisco, J. S.: Red-light-induced decomposition of an organic peroxy radical: a new source of the HO₂ radical, *Angew. Chem. Int. Ed.*, 54, 15711-15714, <https://doi.org/10.1002/anie.201509311>, 2015.
5. Bianchi, F., Kurten, T., Riva, M., Mohr, C., Rissanen, M. P., Roldin, P., Berndt, T., Crounse, J. D., Wennberg, P. O., Mentel, T. F., Wildt, J., Junninen, H., Jokinen, T., Kulmala, M., Worsnop, D. R., Thornton, J. A., Donahue, N., Kjaergaard, H. G., and Ehn, M.: Highly oxygenated organic molecules (HOM) from gas-phase autoxidation involving peroxy radicals: a key contributor to atmospheric aerosol, *Chem. Rev.*, 119, 3472-3509, <https://doi.org/10.1021/acs.chemrev.8b00395>, 2019.